Battery and Ultracapacitor Combinations – Where Should the Converter Go?

John M. Miller
Maxwell Technologies, San Diego, CA
jmiller@maxwell.com

Gianni Sartorelli
Maxwell Technologies, Rossens, CH
gsartorelli@maxwell.com

Abstract- **This paper is focused on what is being referred to now as the hybridized battery. Hybridized energy storage at the package level entails combination architectures of battery and capacitor enabled with a power electronic converter. The introduction of power electronics into the energy storage component mix brings with it considerable flexibility in decoupling the power and energy functions of storage but also introduces the new feature of advanced energy management directly into the storage system. The benefits of power electronic enabled energy storage are numerous and include greater flexibility in meeting individual application demands for burst power and for sustained energy all the while subject to an OEM specific energy management strategy. Power electronic managed energy storage not only decouples power and energy but facilitates improved reliability and life for cold temperature performance; enables the separation of Joule losses, moved from the battery and minimized in the ultracapacitor; presents the opportunity to introduce a true energy battery at lower cost/Wh without loss of high burst power; enhances the capability of energy storage to source and sink high power at end of life without over sizing the battery; sustains the capability of the energy storage to fully recuperate braking energy in a vehicle when cold and when the battery is at high state of charge.**

I. Introduction

There has been a lot of work in recent years on using ultracapacitors to augment batteries and to hybridize the battery via the introduction of power electronics to manage energy and control power levels. R.King, et.al.,[1] develop a dc-dc converter to evaluate an ultracapacitor-battery combination having the following requirements and performance attributes.

TABLE I
Bidirectional Half-H dc-dc Converter to Interface an Ultracap to Battery

Requirements and results	Peak power (kW)	Min	Max
Dc link voltage, battery-inverter	25	300V	400V
Converter input voltage swing		150V	300V
Converter efficiency/Power level		95.3%	98.4%
Converter input current level		83A	167A

In Table I the battery is a 20kWh, 336V unit. System peak power is 65kW @ 80% DOD. Dixon, et.al., [2] describe a similar implementation of ultracapacitor plus dc-dc converter in active parallel with a traction battery as the energy storage unit for an all electric Chevy S-10 pick-up truck. In this system some basic control implementations are given to manage the energy level of the ultracapacitor bank, a 360V, 7F, 45kg pack. With the converter and controller the total capacitor plus converter package mass is 70kg. The battery pack is comprised of 26 valve regulated lead acid (VRLA) 12V modules having an open circuit voltage of 312V.

Pesaran, et.al., [3] describe the use of ultracapacitors in an energy recuperating micro-hybrid as being likely in the near term and as possible if used in combination with VRLA batteries. For mild-hybrids the authors cite the situation as not possible if the engine is downsized, but as possible in combination with VRLA or other battery type. More recently Gonder and Pesaran [4] have reported on the integration of ultracapacitors only energy storage in the GM Saturn Vue Greenline mild-hybrid vehicle and go on to demonstrate performance that is on par with the production nickel-metal-hydride (NiMH) 42V pack.

The introduction of ultracapacitors into mainstream automotive traction applications is beginning to gain acceptance when various investigators across the globe are finding the same results, that highly cyclable energy storage afforded by the ultracapacitor is well suited to vehicle traction applications.

II. Power Electronic Enabled Hybrid Battery

The real enabler for hybridized energy storage systems is power electronics. Over the years vehicle manufacturers and universities have done considerable research in electric energy storage systems that are best suited to vehicle use. Verbrugge, et.al.,[5] discuss the energy storage requirements for a range extended vehicle, such as the Chevy Volt plug-in hybrid electric vehicle (PHEV), as a potential candidate for battery-capacitor combinations. In this work the authors describe the tandem connection of six 100F ultracapacitors across the series connection of two 8.5Ah lithium-ion cells and show that such a combination offers promise over present state-of-art advanced batteries alone. To quantify potential service life enhancement of the combination the lithium-ion cell, its temperature can be used as a surrogate for battery life. The tandem connection is the simplest approach to battery-capacitor combinations, but because of voltage clamping by the battery it has inferior performance to the active combination realized by judicious application of power electronics – but what is an optimal configuration and power rating? These questions are discussed in detail below.

A. *Power Converter Essentials*

Before proceeding on to the preferred or optimum architecture for active combination technologies it is beneficial to investigate the basic principles of dc-dc power converter operation. There is no question today that the inductor input, single phase leg, mid-point or half-H converter, is the best option for a non-isolated, bi-directional, buck-boost converter to interface an ultracapacitor to a battery. Schupbach and Balda, [6] discuss the development of a 35kW half-H dc-dc converter as the best choice for this application by placing special emphasis on the stress levels that the wide input voltage swing will have on the converter components. Their conclusion: the half-H, inductor input converter is optimum for such use. The architecture of the ultracapacitor and battery in active combination using the inductor input half-H converter is shown as Fig. 1. The two filtering capacitors, C_1 and C_2, are needed to limit high frequency switching current leaking to the ultracapacitor and to the battery respectively.

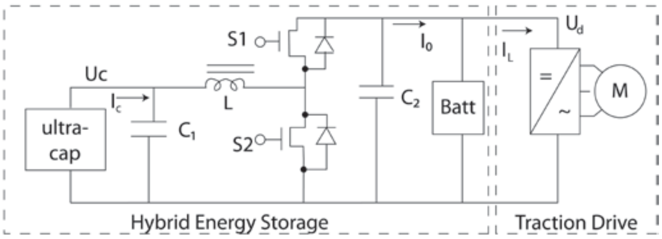

Fig. 1. Architecture of Active Combination of Ultracap with Battery

It is important to point out that the active combination architecture shown as Fig. 1 is not limited to only ultracapacitor voltage below battery voltage, but that this architecture is equally applicable to the case for ultracapacitor voltage greater than the battery voltage, just not identical to the battery voltage. The reason for this can be seen by examining (1) as the definition for boost duty cycle, d_1, and buck duty cycle, d_2, and (2) for the case of boosting the ultracapacitor voltage to the top of its voltage window: $U_c=U_{mx}/2$ to U_d, when $U_{mx} = U_d$ for the case of ultracapacitor voltage and battery voltage being nearly on par result in the limits shown in (2) and (3), which are also summarized in Table II.

$$d_1 = 1 - \frac{U_c}{U_d} = (1-d_2) = \frac{U_d - U_c}{U_d} \quad (1)$$

$$0 \le d_1 = 1 - \frac{U_c}{U_d} \le 0.98 \quad (2)$$

$$0.05 \le d_2 = \frac{U_c}{U_d} \le 0.5 \quad (3)$$

TABLE II

IDEAL CONVERTER INPUT-OUTPUT PARAMETERS UNDER POWER INVARIANCE: I_C=INVERTER INPUT CURRENT, I_0=CONVERTER OUTPUT CURRENT, U_D=DC LINK VOLTAGE TO TRACTION INVERTER. I_L=TRACTION INVERTER INPUT CURRENT

Converter mode	Ultracap voltage, U_c U_c=	Ultracapacitor current, I_c I_c=	Output power $P_o = U_cI_c$=
Buck	d_2U_d	$\left(\frac{1}{d_2}\right)I_0$	U_dI_0
Boost	$(1-d_1)U_d$	$\frac{1}{(1-d_1)}I_0$	U_dI_0

If the maximum ultracapacitor voltage, $U_{cmx}=U_d/2$, then $U_{cmn}=U_d/4$ then the limits on duty cycle set by (2) and (3) become $\{0.5<d_1<0.75\}$ and $\{0.25<d_2<0.5\}$, and so on for any other condition on ultracapacitor voltage relative to the battery voltage.

In [7] these same authors specify the minimum input inductor value according to the relations in (4) and for which we specify a switching frequency f_s=20 kHz (in some designs 50kHz or even 250kHz), a peak-peak inductor ripple current δI_c=0.3pu, and input and output voltage ripple $\delta U_c = \delta U_d$=0.05pu respectively. There is currently on-going investigation to quantify the limits on tolerable ripple current and voltage for the ultracapacitor (and for the battery) in such combination architectures. In particular, the minimum ratings for converter input ripple filter capacitor, C_1, and output ripple filter capacitor, C_2, both of which must be high quality film or ceramic types.

$$L_{mn} = \max\left\{\frac{U_d d_1(1-d_1)}{\delta I_c f_s}; \frac{U_d d_2(1-d_2)}{\delta I_c f_s}\right\} \quad (4)$$

B. InductorInput half-H Converter

To illustrate the performance of the dc-dc converter a simulation is run with parameters for C_1 and C_2 from [7] and the inductor value of 58μH calculated from (4). The example implements the architecture of Fig. 1 using the parameters of a Maxwell BMOD015-P048 ultracapacitor module (165F, 48V) and a regulated output voltage of $72V_{dc}$. The converter output load is taken as a constant 518W local load plus a time dependent current load due to the traction drive shown. Figure 2 summarizes the performance of this converter for a constant load, I_L=50A, plus the local load of 7.2A.

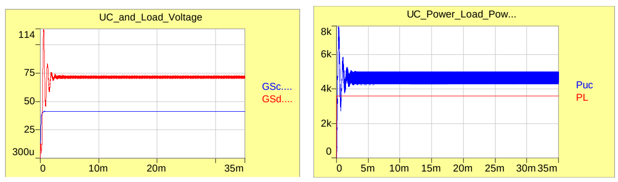

Fig. 2. Simulation of dc-dc converter of Fig.1 for active combination. Response to 50A constant load current: Left, voltages ultracap at 42V and converter output at 72V; Right, converter input power 4.6kW, a 0.528kW local load plus 50A dc load at 3.6kW. Current band of 15App (C_1=0.11uF, C_2=100uF, L=58uH, fs=20kHz, and δI=15App)

The transient performance of the dc-dc converter operating in boost mode is illustrated further in Fig. 3 for the same example of a 48V ultracapacitor module at ~77% SOC as it would be if used in a micro or mild hybrid electric vehicle. The duty cycle regulator for the converter is implemented as a comparison of voltage to a sawtooth wave to generate a PWM switching pattern to the half-H lower switch (S2 in Fig. 2). Only in this case the load current is set to the transient condition of a 100A step at t=7ms followed by a further step to 225A at t=16ms. Current pulse rise time is set to 400us and the time axis is compressed for reasonable computer time for high frequency switching. Load power at the 72V regulated output voltage and 225A is 18.6kW.

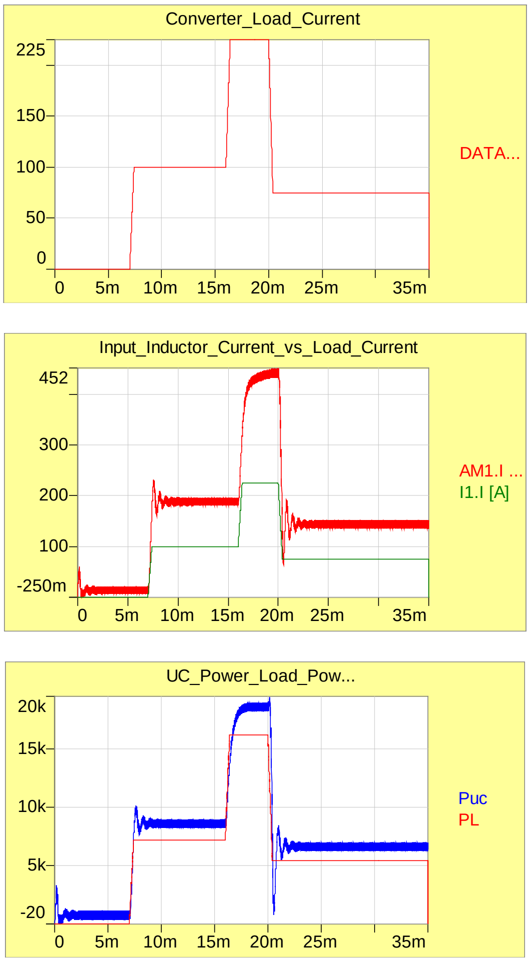

Fig. 3. Simulation of dc-dc converter of Fig.1 for active combination. Transient response case: Top, applied load current at 72V bus; Center, converter input inductor current; Bottom, ultracap power output is approx 18.6kW versus load power output 16.2kW (plus 0.518kW local load).

In Fig. 3 the ultracapacitor power is higher than the load power for two reasons: 1) constant load current at a regulated voltage dc bus applies constant power to the ultracapacitor, and 2) the internal resistance, ESRdc, of the ultracapacitor contributes significant loss at such high power levels. In this case, the internal dissipation of the ultracapacitor, measured when t=18ms in Fig. 3, is 1.622kW. At this same point the dissipation in a load resistance on the 72V dc bus is 1.251kW peak and 632W peak in the electronic switch. The load losses are therefore $(1-d_1)*P_{diode} + d_1*P_{RL} = 0.415*632 + 0.585*1251 = 994W$. Total losses are therefore approximately 2.616kW when t=18ms. The ultracapacitor, converter and system efficiency are therefore:

$$\eta_{uc} = \frac{1}{\left(1+\dfrac{P_{disp}}{P_{uc}}\right)} = \frac{1}{\left(1+\dfrac{1.622}{18.6}\right)} = 0.92 \quad (5)$$

$$\eta_{conv} = \frac{1}{\left(1+\dfrac{(d_1 P_{disp\_conv})}{P_{conv}}\right)} = \frac{1}{\left(1+\dfrac{0.415(0.632)}{16.2}\right)} = 0.984 \quad (6)$$

$$\eta_{sys} = \eta_{uc}(\eta_{conv}) = 0.92(0.984) = 0.905 \quad (7)$$

A design principle to follow when interfacing an ultracapacitor to a battery in the active parallel configuration requires the ultracapacitor branch, including its power electronics, possess system efficiency greater than 90%. The second criteria requires that the converter dynamic response be sufficiently fast to accommodate any load transient. Figure 4 is a zoomed portion of the load current transition shown in Fig. 3 at t=7ms. In this figure the individual switching events in inductor current are apparent as well as the $\delta I \sim 17A_{pp}$.

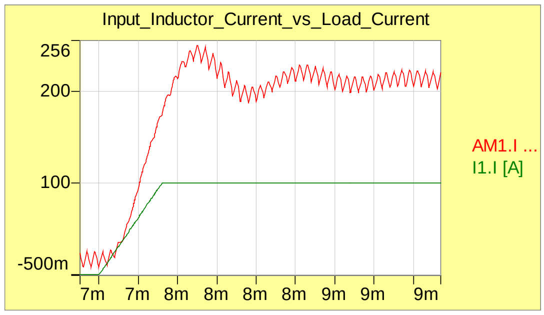

Fig. 4. Simulation of dc-dc converter of Fig.1 for active combination. Transient response case zoomed at t=7ms showing converter response to a 225A current pulse.

III. Architecting the Optimum Architecture

Miller and Smith in [8] describe alternative ultracapacitor-battery combinations designed to optimize the delivery of power to an actuator such as an electric motor drive, engine starter motor, or other actuator. This parallel and cascade architecture are ideal for delivering voltage to a load that is fractionally higher than the battery voltage itself, for example, 16V to a 12V starter motor to boost power at cold temperature, or 16V to an electric assist steering motor. Figure 5 gives an illustration of the parallel boost and cascade boost configurations considered. In the parallel boost configuration and for an electric actuator having substantial current demand from the vehicle electrical distribution system the line impedance, Z_{line}, between the actuator and the vehicle battery-alternator source may result in a voltage drop that reduces actuator performance, for example electric power steering or vehicle rear steering actuators. In this case the introduction of an ultracapacitor distributed module, a small charge pump (power electronic converter) and steering diode insure that an actuator that requires 14.2V nominal is supplied with this voltage (or somewhat higher voltage) without being encumbered by line loss. The cascade configuration shown in Fig. 5, also referred to as pseudo-42V PowerNet when the ultracapacitor distributed module is rated 24V and is series connected with the vehicle battery. In this system a boost converter draws power from the vehicle power supply and maintains the distributed module at the appropriate voltage for the actuator, shown here as the 14.2V nominal load controller and actuator (the ultracapacitor module in this case may be only a 2 cell string operating at a nominal 4V). In the cascade architecture the full load current passes through the battery and the ultracapacitor cells.

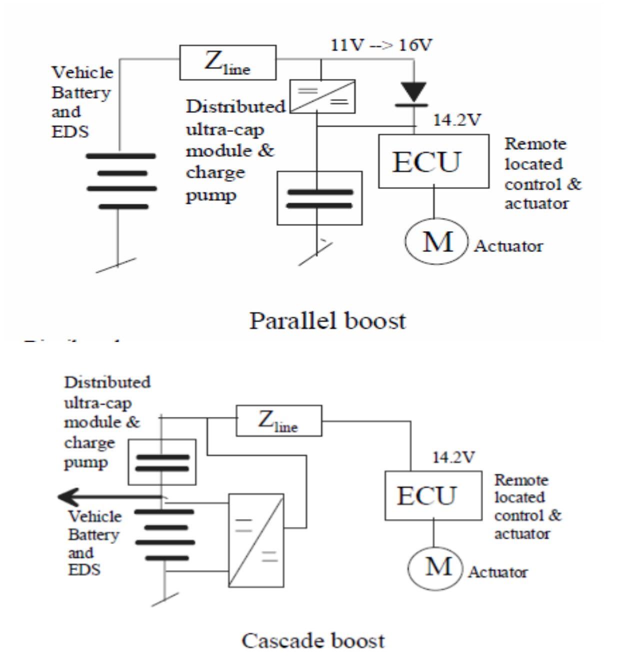

Fig. 5. Parallel and cascade architecture for boosting voltage delivery to a load [8](Top: parallel boost, Bottom: cascade boost)

In [9] Guidi and Undeland continue the investigation of cascaded architectures by constructing a half controlled cascade architecture having minimum power electronic content shown in Fig. 6. In this power electronic configuration the premises is that it is possible to have an uncontrolled voltage (potential across SC_0) in series with a controlled potential, managed by the power converter interfacing ultracapacitor SC_1 and use this controllable potential to make up the difference between the battery potential and the uncontrolled ultracapacitor, SC_0. This is demonstrated to be feasible for 50% charge cycling of the ultracapacitors when $SC_0 = 3SC_1$ so that both ultracapacitors in series are available via the fractional pu converter to match the battery voltage.

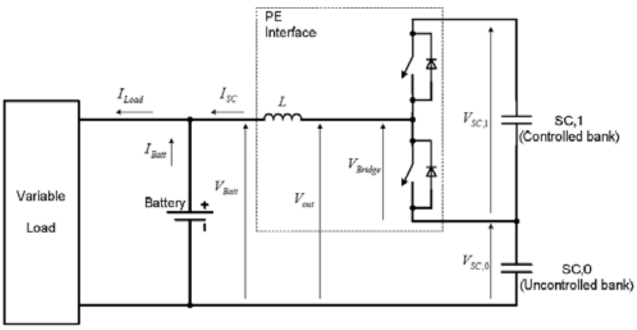

Fig. 6. Half controlled cascaded ultracapacitor architecture [9]

Other architectural implementations are being evaluated by researchers around the globe. Reference [10] describe a hybrid energy storage pack in which the converter manages battery and ultracapacitor charge level according to the load requirements while delivering high pulse power and having optimum energy density battery as shown in Fig. 7.

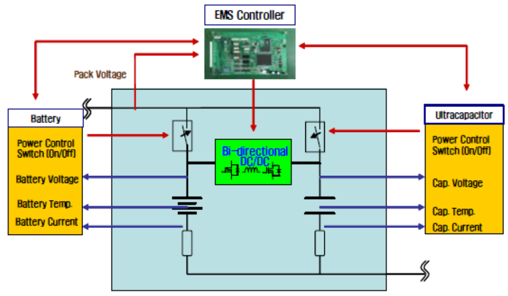

Fig. 7. Hybrid energy pack configuration with energy optimized battery and high power ultracapacitor [10]

The switching configuration shown in Fig. 7 makes it possible to access the energy component, the battery, independently of the power component the ultracapacitor. For this configuration, like the half-controlled cascade shown in Fig. 6, the power electronic converter is rated 0.5pu or lower. This provides a cost opportunity in implementation.

IV. Frequency Response of the Hybridized Battery

This section will discuss the frequency response of a system consisting of a battery actively coupled to an ultracapacitor and present some results. Indeed what behavior can we expect from a such hybrid when stressed at high cycle rate or high frequency? Considerable effort has gone into EIS – electrochemical characterization of the ultracapacitor and the influence frequency has on ESR and capacitance. Figure 8 illustrates these effects, made from laboratory measurement of ultracapacitor cells, as characterization of ESR and capacity trends versus cell potential with frequency as a parameter. Ultracapacitor ripple current (see Fig. 3) falls into this category of frequency effects and is the subject of on-going experiment.

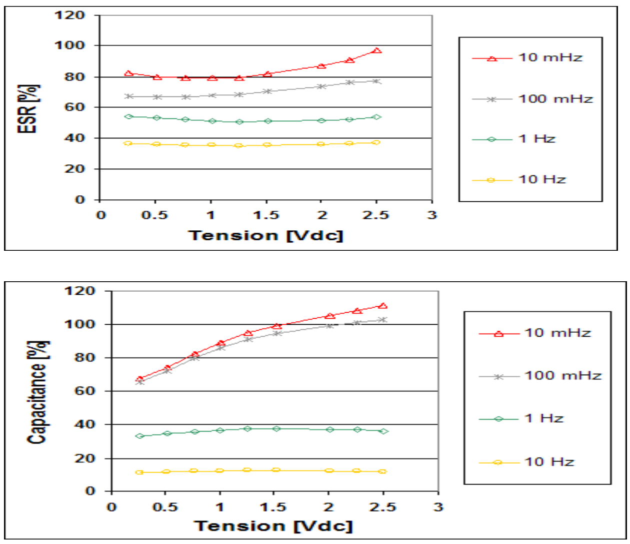

Fig. 8. Variation of ultracapacitor parameters with cell potential and frequency as a parameter

V. Application to Electric Vehicles

This section will examine the placement of the bidirectional dc-dc converter on the battery with ultracapacitor tied directly to the traction drive inverter and a second configuration where the converter interfaces the ultracapacitor to the traction drive inverter. The first case is a variable dc link voltage implementation and the second case is that of fixed dc link voltage [11]. For the architecture of the first case the inverter voltage modulator must accommodate a highly variable dc link whereas in the second architecture the inverter voltage modulator must deal with only modest variability of the dc link voltage. The question is, which architecture is best for active combination energy storage systems? To answer this, a battery electric vehicle is evaluated for each of three cases:

- Converter on the battery with ultracapacitor alone supporting the dc link voltage. This is the floating dc link architecture and an implementation that requires innovation in the energy management strategy.
- Converter on the ultracapacitor, sub-case having ultracapacitor voltage lower than dc-link. This is the up-convert case, and
- Converter on the ultracapacitor, sub-case having ultracapacitor voltage greater than dc-link. This is the down convert case.

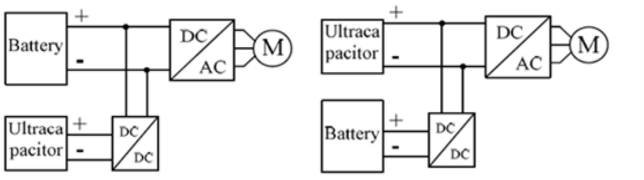

Fig. 9 Architectures to be evaluated as optimum for electric vehicle application: Left, converter on the ultracapacitor in fixed dc-link voltage implementation and Right, converter on the battery yielding a floating dc-link voltage implementation.

Details of the implementation can be found in [11]. For our purposes here the illustration in Fig. 10 shows how the active combination is configured along with an energy management strategy to manage power flows and to maintain the ultracapacitor SOC_{uc} within the range: $0.25<SOC_{uc}<1.0$.

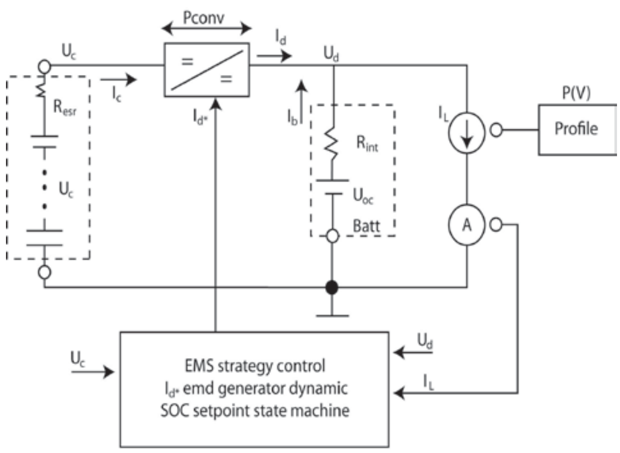

Fig. 10 Architecture of two implementation cases having dc-dc converter on the ultracapacitor (up-convert and down-convert cases). For the BEV studied the battery is 28kWh lithium-ion and the ultracapacitor has 78Wh energy, 58Wh of which is useable.

Figures 11 and 12 summarize the BEV example in terms of converter power, ultracapacitor SOC_{uc} variation, the constraint that SOC_{uc} remain within its operating window plus battery rms current and its spectrum for comparisons.

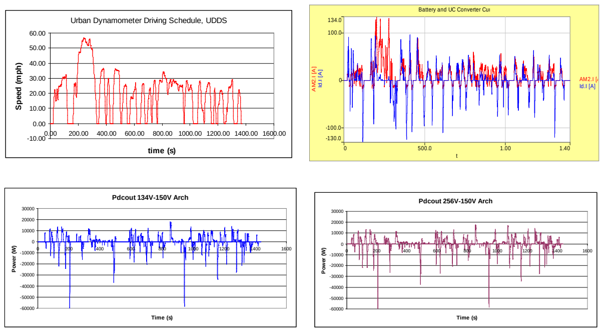

Fig. 11 Performance of the active combination in a BEV over the UDDS drive cycle. Top: UDDS velocity vs. time and converter output current vs. battery current, Bottom: dc-dc converter power up-convert (lower left) and down convert (lower right).

Performance of the converter in both up-convert and down-convert cases for the converter on the ultracapacitor is clearly evident from Fig. 12. In this figure the spectrum of converter output power is shown only for the up-convert and the converter on the battery case, since the down-convert case is so similar to the up-convert case.

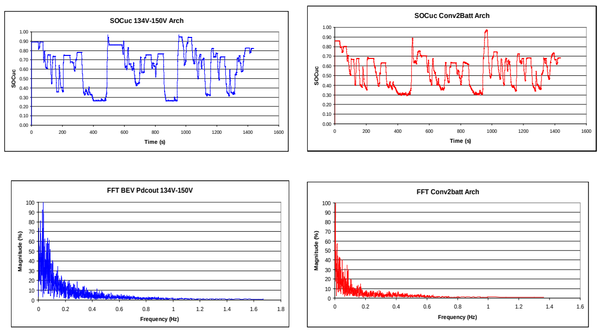

Fig. 12 Performance of the active combination in a BEV over the UDDS drive cycle (up-convert on left, converter on battery on right). Top: SOC_{uc} variation over the complete 1340s cycle, Bottom: Spectrum of dc-dc converter output power.

Note that in Fig. 12 the SOC_{uc} when the converter is on the battery is a somewhat shallower window that for the up-convert and down-convert cases. This is because the energy management strategy (EMS) used in the converter on the battery case is significantly different than for the up- or down-convert cases. For both of the fixed dc-bus cases the same EMS strategy applies, and that is to maximize use of available ultracapacitor energy. For the converter2battery case the EMS relies on inverse logic, that is, the battery only contributes when the ultracapacitor can no longer support boosting power and the battery contribution is zero when the vehicle is in regeneration mode. The FFT plots in Fig. 12 show that the EMS for the converter to battery case is less populated due to less activity than for the converter to ultracapacitor case.

VI. CONCLUSION

The inclusion of a power electronic converter into the energy storage system to truly decouple power and energy has been discussed in detail. We refer to the optimal implementation of ultracapacitor and battery as the eclectic principle. Basically, there are five key assertions to the eclectic principle:

- Improved reliability and life for cold weather performance,
- Full energy capture during vehicle regeneration at high ESS SOC,
- Full power delivery capability at end-of-life (EOL) without over-sizing the battery,
- Combination architectures permit the use of higher specific energy ESS technology, lower cost/Wh, and higher power,
- Segregation of I^2R Joule losses, shifted from the battery, minimized with ultracapacitors.

Overall, the benefits of the three architectures discussed for application to the ESS in a battery-EV can be summarized as shown in Table III. This Pugh analysis ranks the combination technology on robustness, implementation cost, performance and overall score.

TABLE III
ACTIVE PARALLEL COMBINATION ARCHITECTURES COMPARED

Architecture	Robustness	Cost	Performance	Overall
Up Convert	Fewer, large UC cells, few conn's High input current to converter Stable dc link	1 Lower voltage semiconduct	1 Converter operates only when needed High bandwidth control	+ Best choice overall and considering PE technology advances
Down Convert	More, smaller UC cells, more conn's Lower input current Stable dc link	0 high voltage semiconduc	1 Converter operates only when needed High bandwidth control	0 Too many interconnects, voltage management, higher voltage UC system
Converter on Batt	More, smaller UC cells, more conn's Highly dynamic dc link voltage Difficult Inverter PWM control	-1 Converter operational 100% of time Thermal concerns	0 Converter fault cannot be tolerated Higher thermal burden	- Requires ultra-robust converter and high performance inverter controller and higher current inverter switch

Table III answers the question posed in the title to this paper, where should the converter go? The converter should go on the ultracapacitor and its implementation is best when up-converting from lower voltage capacitors to a higher voltage dc-bus.

Future work consists of experimental design and testing of the topics of section IV on power electronic induced switching frequency effects on electrochemical storage components.

ACKNOWLEDGMENT

The authors acknowledge the support of Maxwell Technologies in the preparation of this paper and also for on-going outside testing of converter ripple current effects on ultracapacitor parameters. Results of this testing will be described in a future paper. Special thanks go to Ted Bohn of Argonne National Laboratory for on-going discussion, support and for the reality checks on combination technology noted in the conclusions.

REFERENCES

[1] R.D. King, J. Schwartz, M. Cardinal, L. Salasoo, N. Garrigan, "Development and System Test of a High Efficiency Ultracapacitor/Battery Electronic Interface," The International Battery, Hybrid and Fuel Cell Electric Vehicle Symposium, EVS15, May 1999

[2] J.W. Dixon, M. Ortuzar, E. Wiechmann, "Regenerative Braking for an Electric Vehicle Using Ultracapacitors and a Buck-Boost Converter," The International Battery, Hybrid and Fuel Cell Electric Vehicle Symposium

[3] A. Pesaran, T. Markel, M. Zolot, S. Sprik, "Ultracapacitors and Batteries in Hybrid Vehicles," Advanced Capacitor World Summit, ACWS2005, Hilton San Diego Resort, San Diego, CA, 11-13 July 2005

[4] J. Gonder, A. Pesaran, J. Lustbader, H. Tataria, "Hybrid Vehicle Comparison Testing using Ultracapacitors vs. Battery Energy Storage," SAE 2010 Hybrid Vehicle Technologies Symposium, Double Tree Hotel, San Diego, CA 10-11 Feb. 2010

[5] M. Verbrugge, P. Liu, S. Soukiazian, R. Ying, "Electrochemical Energy Storage Systems and Range-Extended Electric Vehicles," The 25th International Battery Seminar & Exhibit, Broward County Convention Center, Ft. Lauderdale, FL, March 2008

[6] R.M. Schupbach, J.C. Balda, "35kW Ultracapacitor unit for Power Management of Hybrid Electric Vehicles: Bi-directional dc-dc Converter Design," The 35th IEEE Power Electronics Specialists Conference, PESC2004, Aachen, Germany

[7] R.M. Schupbach, J.C. Balda, "Comparing dc-dc Converters for Power Management in Hybrid Electric Vehicles," IEEE International Electric Machines and Drives Conference, IEMDC'03, Madison, WI, Vol.3, pgs 1369-1374, 1-4 June 2003

[8] J.M. Miller, R.M. Smith, "Ultracapacitor Assisted Electric Drives for Transportation," IEEE International Electric Machines and Drives Conference, IEMDC'03, Madison, WI, Vol.3, pgs 1369-1374, 1-4 June 2003

[9] G. Guidi, T.M. Undeland, Y.Hori, "An Interface Converter with Reduced VA Ratings for Battery-Supercapacitor Mixed Systems," IEEE Power Conversion Conference, PCC07, Nagoya, Japan, April 2007

[10] B-H. Lee, D-H. Shin, B-W. Kim, H-J. Kim, B-K. Lee, C-Y. Won, J. Hur, "A Study on Hybrid Energy Storage System for 42V Automotive PowerNet," IEEE VPPC'06, Windsor, UK, Sept. 2006

[11] J.M. Miller, "Engineering the Optimum Architecture for Storage Capacitors," Advanced Automotive Battery Conference, AABC2010, Large EC Capacitor Technology and Application, ECCAP, Session 3, EC Capacitor Storage System Applications, Omni Orlando Resort, 18-21 May 2010